Neurobiology of Aging 80 (2019) 210–222

Contents lists available at ScienceDirect

Neurobiology of Aging

journal homepage: www.elsevier.com/locate/neuaging

Age-dependent alterations of Kir4.1 expression in neural crest–derived cells of the mouse and human cochlea

Ting Liu [a,d,1], Gang Li [a,e,1], Kenyaria V. Noble [a], Yongxi Li [d], Jeremy L. Barth [b], Bradley A. Schulte [a,c], Hainan Lang [a,*]

[a] Department of Pathology and Laboratory Medicine, Medical University of South Carolina, Charleston, SC, USA
[b] Department of Regenerative Medicine, Medical University of South Carolina, Charleston, SC, USA
[c] Department of Otolaryngology-Head and Neck Surgery, Medical University of South Carolina, Charleston, SC, USA
[d] Department of Otolaryngology Head and Neck Surgery, Beijing Tongren Hospital, Capital Medical University, Key Laboratory of Otolaryngology Head and Neck Surgery, Ministry of Education, Beijing, China
[e] Department of Otolaryngology, Tinnitus and Hyperacusis Center, Yueyang Hospital of Integrated Traditional Chinese and Western Medicine Affiliated to Shanghai University of Traditional Chinese Medicine, Shanghai, China

ARTICLE INFO

Article history:
Received 29 December 2018
Received in revised form 2 April 2019
Accepted 11 April 2019
Available online 18 April 2019

Keywords:
Presbyacusis
Human temporal bone
Neural crest–derived cells
Kir4.1
Auditory nerve
Stria vascularis
Spiral ganglion

ABSTRACT

Age-related hearing loss (or presbyacusis) is a progressive pathophysiological process. This study addressed the hypothesis that degeneration/dysfunction of multiple nonsensory cell types contributes to presbyacusis by evaluating tissues obtained from young and aged CBA/CaJ mouse ears and human temporal bones. Ultrastructural examination and transcriptomic analysis of mouse cochleas revealed age-dependent pathophysiological alterations in 3 types of neural crest–derived cells, namely intermediate cells in the stria vascularis, outer sulcus cells in the cochlear lateral wall, and satellite cells in the spiral ganglion. A significant decline in immunoreactivity for Kir4.1, an inwardly rectifying potassium channel, was seen in strial intermediate cells and outer sulcus cells in the ears of older mice. Age-dependent alterations in Kir4.1 immunostaining also were observed in satellite cells ensheathing spiral ganglion neurons. Expression alterations of Kir4.1 were observed in these same cell populations in the aged human cochlea. These results suggest that degeneration/dysfunction of neural crest–derived cells maybe an important contributing factor to both metabolic and neural forms of presbyacusis.

© 2019 Elsevier Inc. All rights reserved.

1. Introduction

Age-related hearing loss (presbyacusis) is a global public health problem that impacts the well-being of many elderly people. Presbyacusis is characterized by declines in hearing sensitivity and understanding of speech, especially in noisy environments, slowed central processing of acoustic information, and impaired localization of sound sources (Gates and Mills, 2005). Overall, about 30% of Americans aged 65–74 and 50% of those over 75 have impaired hearing (Gates and Mills, 2005). There are at least 3 types of presbyacusis - sensory, strial (or metabolic) and neural - which can occur alone or together in individual subjects. Studies of human temporal bones (HTBs) strongly indicate that presbyacusis, in the absence of significant noise trauma, stems from degeneration/dysfunction of nonsensory regions of the cochlea, such as in the stria vascularis (STV) and auditory nerve rather than sensory hair cells in the organ of Corti (OCT) (Gates and Mills, 2005; Kusunoki et al., 2004; Makary et al., 2011; Schuknecht and Gacek, 1993; Suzuki et al., 2006). In the mammalian cochlea, several types of nonsensory cells including strial intermediate cells and fibrocytes in the lateral wall and glial cells in the auditory nerve are capable of regeneration under stressful conditions, although their ability to repopulate/self-repair declines with age (Lang et al., 2003, 2011; Yamasoba et al., 2003). Neural crest cell lineages give rise to several types of nonsensory cells in the inner ear, including strial intermediate cells, mesenchymal cells in the spiral ligament, and glial cells of the auditory nerve (Dupin and Sommer, 2012; Hilding and Ginzberg, 1977; Locher et al., 2014). Previous studies in animal models have demonstrated that degeneration of the cochlear lateral wall and a corresponding reduction in the endocochlear potential (EP) play a prominent role in presbyacusis (Lang et al., 2010; Schmiedt, 1996, 2009; Schmiedt et al., 1996; Schulte and Schmiedt, 1992; Spicer et al., 1996). In this study, we evaluated the hypothesis that degeneration/dysfunction of neural

* Corresponding author at: Department of Pathology and Laboratory Medicine, Medical University of South Carolina, 165 Ashley Avenue, PO BOX 250908, Charleston, SC 29425, USA. Tel: +1 843-792-2711; fax: +1 843-792-0368.
E-mail address: langh@musc.edu (H. Lang).
[1] These authors contributed equally.

0197-4580/$ – see front matter © 2019 Elsevier Inc. All rights reserved.
https://doi.org/10.1016/j.neurobiolaging.2019.04.009

crest–derived cells in the cochlear lateral wall and auditory nerve is associated with presbyacusis using both a CBA/CaJ mouse model and temporal bones obtained from human donors.

Inwardly rectifying potassium (Kir) channels are present in a wide variety of cell types and play critical roles in regulating many cellular activities including signaling processes, resting membrane potentials, neurotransmitter release and neuronal excitability, electrolyte transport in epithelial cells, and cellular contraction and volume changes (Chen and Zhao, 2014; Shieh et al., 2000). Kir channels are divided into 7 subfamilies (Kir1.0-Kir7.0) and include more than 20 members based on their molecular and electrophysiological characteristics. The expression of Kir4.1 *(KCNJ10)* was first reported in glial cells of the central nervous system and then in the kidney, retina, and inner ear (Bond et al., 1994; Garcia et al., 2007; Hibino et al., 1997). In the mammalian cochlea, Kir4.1 is expressed in the cochlear lateral wall, satellite cells surrounding spiral ganglion neurons (SGNs), and supporting cells in the OCT (Ando et al., 1999; Hibino et al., 1997; Jagger et al., 2010; Kim et al., 2013; Rozengurt et al., 2003). It is believed that Kir4.1 expression in the cochlea is necessary for (1) generation and maintenance of the EP and the high K^+ concentration in the endolymph and (2) buffering by satellite cells of K^+ ions expelled from neurons during excitation in the auditory nerve (see review by Chen and Zhao, 2014). In the central nervous system, dysregulation of astroglial Kir4.1 has been reported to occur in animal models representing a wide array of neurological diseases such as Huntington's disease (Tong et al., 2014), Rett syndrome (Lioy et al., 2011), and depression (Cui et al., 2018). Astroglial Kir4.1 also is dysregulated in older mice subjected to traumatic brain injury (Gupta and Prasad, 2013). In this study, we examined changes in the pattern and levels of Kir4.1 expression to determine the functional integrity of neural crest–derived cells with age in cochleas obtained from CBA/CaJ mice and HTBs.

2. Materials and methods

2.1. Animals

CBA/CaJ mice have been widely used as a model to study late-onset hearing loss (Ohlemiller, 2009; Ohlemiller et al., 2010). For this study, CBA/CaJ mice were divided into 2 groups; young adult (1.5–3 months old) and aged (1.5–2.5 years old). The groups included both sexes. The mice were derived from breeders purchased from The Jackson Laboratory (Stock number: 000654; Bar Harbor, ME). The animals were bred and housed in a low-noise environment and maintained on a 12-h light/dark cycle at the animal research facility of the Medical University of South Carolina (MUSC). All procedures were conducted in accordance with the guidelines of MUSC's Institutional Animal Care and Use Committee.

2.2. Measurement of auditory brain stem response and endocochlear potential

Auditory brain stem response (ABR) measurements were performed on all mice before sacrifice. The mice were anesthetized by intraperitoneal injection with a mixture of xylazine (20 mg/kg) and ketamine (100 mg/kg) as described previously (Hao et al., 2014; Panganiban et al., 2018). ABRs were recorded using subdermal needle electrodes at the vertex (+) and test-side mastoid (−), with a ground in the control side leg. Sound pressure levels (SPL) were reduced in 5-dB steps from 90 dB SPL to 10 dB SPL. ABR waveforms and thresholds were analyzed at individual frequencies ranging from 4.0 to 45.2 kHz. ABR wave I thresholds were obtained and defined as the lowest sound levels at which a repeatable wave I signal could be identified in the response waveforms.

The EP was measured in the basal turn of the cochlea. The EP was recorded with a micropipette filled with 0.2 M KCl, yielding an impedance of 25–40 MΩ connected to an electrometer (Duo773; World Precision Instruments, Sarasota, FL) for direct recording of the potential. The micropipette was introduced into the scala media via 30–50 μm holes drilled through the otic capsule in the basal turn.

For each age group, ABR wave I thresholds, the maximum wave I amplitudes and EP values were averaged and mean ± SEM values were calculated and plotted using Origin 6.0 software (OriginLab) and GraphPad Prism (GraphPad Software). Data for ABR wave I thresholds and EP levels were analyzed by Student's unpaired *t*-test or Mann-Whitney test. A value of $p < 0.05$ was considered to be statistically significant. After ABR and EP measures, the mice were deeply anesthetized, and cochlear tissues were collected for gene array, ultrastructural or immunohistochemical analysis as described in the following.

2.3. DNA microarray analysis

Total RNA samples were prepared from the auditory nerve and cochlear lateral wall of young adult and aged mice. Three independent samples consisting of tissue from 6 cochleas were prepared for each group; both groups included male and female mice. The total RNA quality was confirmed by Bioanalyzer, and then samples were processed and hybridized to GeneChip Mouse 430 2.0 microarrays (Affymetrix, Santa Clara, CA) as previously described (Lang et al., 2015; Panganiban et al., 2018). Resulting hybridization data were processed with GeneChip Expression Console software (Affymetrix) to derive Robust Multi-array Average normalized expression intensities (Irizarry et al., 2003) and MAS5 detection calls. Microarray data are deposited with NCBI Gene Expression Omnibus (CLW, accession GSE98070; AN, accession GSE121856). Genes relating to neural crest cell function were assembled by query of the Gene Ontology Database (Ashburner et al., 2000; The Gene Ontology Consortium, 2017_PMID: 27899567) and the WikiPathways database (Slenter et al., 2018). Comparative analyses of neural crest–related genes were conducted using dChip software (Li and Wong, 2001) with $p < 0.05$ (Student's *t*-test, unpaired) interpreted as significant. False discovery rates were estimated by iterative comparisons involving randomized sampling groupings.

2.4. Preparation of mouse cochleas for morphological and histochemical studies

For ultrastructural observation, deeply anesthetized mice were sacrificed by intracardial perfusion of a mixture of 4% paraformaldehyde and 2% glutaraldehyde in 0.1 M phosphate buffer (pH 7.4). After cochlear dissection, the oval and round windows were opened and the same fixative was perfused into the scales through the oval window. The cochleas were subsequently immersed in fixative at 4 °C overnight and decalcified in 0.12 M EDTA for 2–3 days. The same procedure was used to process cochleas for immunohistochemistry, except that the fixative was 4% paraformaldehyde and the total exposure time to fixative was limited to 2 hours. The cochlear tissues were decalcified in EDTA, cryoprotected in 30% sucrose in PBS, and embedded in Tissue-Tek OCT compound.

2.5. Transmission electron microscopy and quantitative analysis of intermediate cell structural integrity

For ultrastructural analysis, mouse cochlear tissues were post-fixed with 1% osmium tetroxide for 1 hour, dehydrated, and embedded in Epon LX 112 resin. Semi-thin sections about 1 μm

thick were cut and stained with toluidine blue. Ultrathin sections were stained with uranyl acetate and lead citrate and examined by electron microscopy as previously described (Lang et al., 2011; Panganiban et al., 2018). Quantitative analysis of intermediate cell structural integrity was performed by measuring the intermediate cell functional area defined as the strial regions occupied by processes of intermediate cells interdigitating with those of marginal cells (the shaded areas in Fig. 1H and I). Approximately 100–600 μm^2 areas (occupying the region from the apex of the marginal cells to the bottom of the basal cell level) were randomly selected from middle turns (n = 6 ears for young adult group and n = 4 ears for aged group). Area measurements were conducted manually with the assistance of the histogram function in Adobe Photoshop CS.

2.6. Collection and processing of human temporal bones

HTBs were selected from a collection obtained as part of a longitudinal study of age-related hearing loss conducted by the Clinical Research Center (P50) at MUSC in partnership with the Carroll A. Campbell, Jr., Neuropathology Laboratory (Brain Bank) at MUSC (Xing et al., 2012; Hao et al., 2014). All procedures used for the

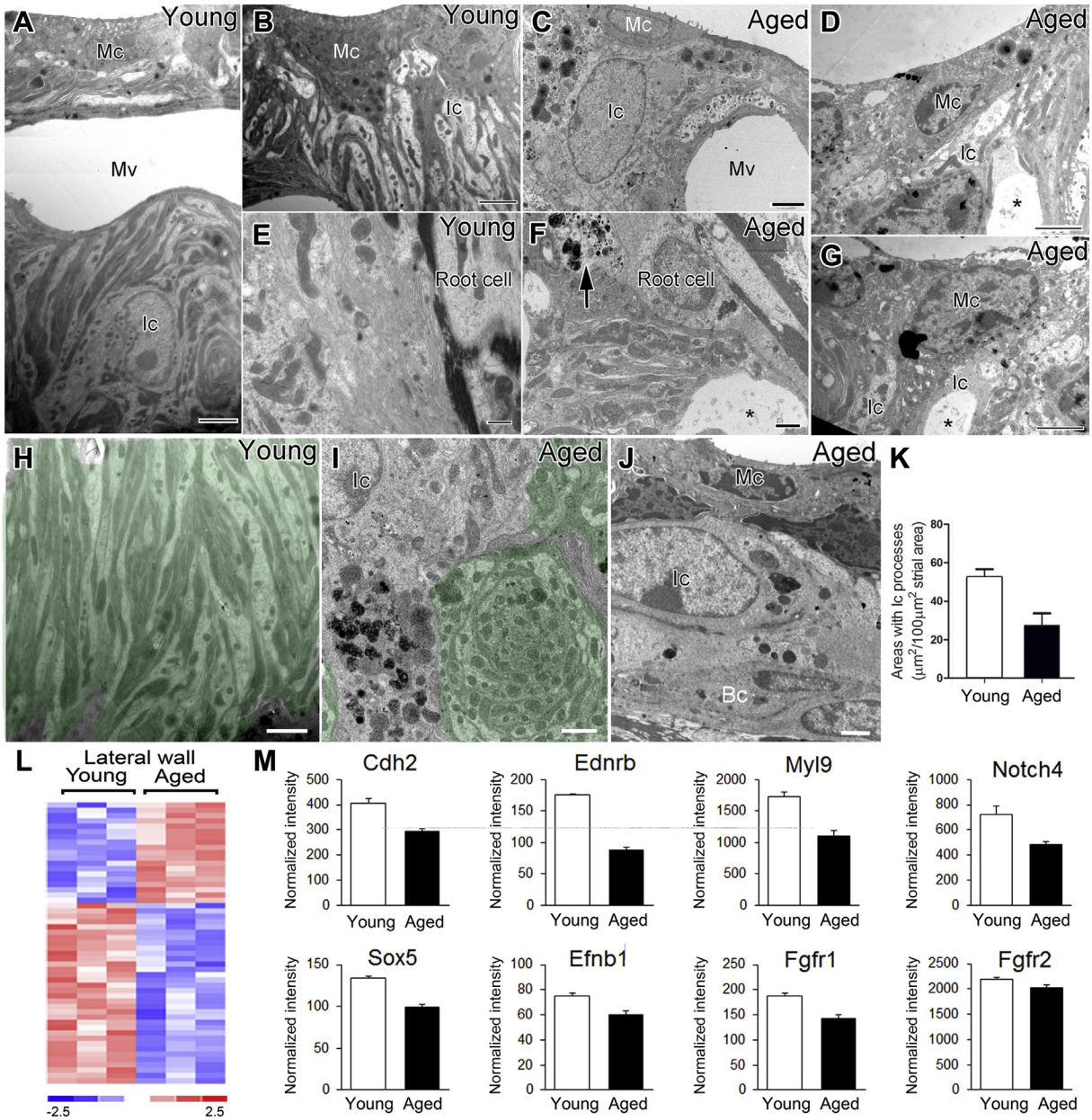

Fig. 1. Age-related alterations in ultrastructure and expression patterns of neural crest–related genes in the mouse cochlear lateral wall. (A–J) TEM images of intermediate cells in the stria vascularis and root cells in the spiral ligament of young (A, B, E, H) and aged (C, D, F, G, I, J) mice. Partial loss (C, D, G, I) or a total loss (J) of the intermediate cell processes, and an increase in cellular debris (arrow) and vacuolization (*) around root cell processes (F) was seen in aged cochleas. Enlarged extracellular spaces (*) between marginal and intermediate cell processes (D, F, G) and abnormal intermediate cell processes (swirl-like structure; I) were often seen in the aged stria vascularis. (K) A significant loss in the area occupied by intermediate cell processes occurred in the aged group compared to young controls (Mann-Whitney test; $p < 0.05$; n = 6 mice for young adult group and n = 4 mice for the aged group). (L) Heatmap of microarray data showing differential expression of 53 neural crest genes in the aged cochlear lateral wall compared with young adult controls ($p < 0.05$; Student's *t*-test, unpaired, 2-tailed, not assuming equal variance). The false discovery rate for this comparison approximated 15%. (M) Microarray expression values are shown for representative neural crest–related genes in the cochlear lateral wall. Scale bar: 2 μm in A, B, C; 1 μm in F; 500 nm in E; 10 μm in D, G; 1.5 μm in H; 800 nm in I; 2 μm in J. Abbreviations: Bc, basal cell; Ic, intermediate cell; Mc, marginal cell; Mv, microvasculature.

harvesting of temporal bones were approved by the MUSC Institutional Review Board under protocol E-607R and Pro00030845, with written consent obtained in all cases. Table 1 lists the age, sex, and postmortem time to fixation for the 12 HTBs used in this study. Immediately after specimen removal (Schuknecht, 1968), the temporal bones were fixed by perilymphatic perfusion with 20 mL of 4% paraformaldehyde solution according to previously described techniques (Hao et al., 2014; Xing et al., 2012). After 48 hours, the perfused temporal bones were rinsed with PBS and decalcified using a microwave-assisted protocol as per our previous description (Cunningham et al., 2001). The total time of decalcification was about 3–6 weeks, and the temporal bones were gradually trimmed to remove most of the hard bone encasing the cochlea and vestibular apparatus.

2.7. Quantitative analysis of Kir4.1 immunoreactivity

Frozen sections of cochlear tissue from mouse and human specimens were incubated overnight at 4 °C with a primary antibody against Kir4.1 (1:100, catalog no: APC035AN0802, Alomone Labs). Secondary antibodies were biotinylated, and binding was detected by labeling with fluorescein isothiocyanate-conjugated avidin D or Texas-conjugated avidin D (Vector Laboratories, Burlingame, CA), and nuclei were then counterstained with propidium iodide or 4′,5-diamidino-2-phenylindole. To further identify cells expressing Kir4.1 as being neural crest derived, dual immunostaining was performed with rabbit anti-Kir4.1 and goat anti-Sox10 (1:100, catalog no: sc173 neural crest–derived 42, Santa Cruz, CA). Areas of interest included STV, root processes (RPs) in the spiral ligament, and the auditory nerve within Rosenthal's canal. Quantitative analysis of Kir4.1 staining intensity was compared by measuring luminescence pixel areas in young adult and aged mouse ears. Confocal images of the Kir4.1 immunostained sections were collected using a Zeiss LSM 880 NLO microscope with ZEN acquisition software (Zeiss). For observations of Kir4.1 expression patterns around SGNs in the mouse, confocal images were collected using either image stacks (Figs. 2 and 3) or a single slice at the depth level, where Kir4.1$^+$ satellite cells were most numerous (Fig. 4). All confocal images of the cochlear lateral wall and the auditory nerve in HTB preparations were taken as image stacks (Figs. 5–7). Image stacks were taken at 0.75 μm intervals with image sizes of 134.95 μm (x) 134.95 μm (y). Images were processed using ZEN 2012 Blue Edition (Carl Zeiss Microscopy), Application Suite X (version 3.0.2.16120; Leica Microsystems), and Photoshop CC (Adobe Systems). Data for Kir4.1 expression intensity are presented as mean ± SEM and analyzed by 2-tailed, unpaired Student's *t*-test (GraphPad Prism). A value of $p < 0.05$ was considered to be statistically significant.

Table 1
Summary of human donor information and Kir4.1 immunoreactivity

ID	Age	Sex	Death to perfusion interval	Kir4.1 immunostaining			
				STV	RP	OCT	RC
H95	30	Male	13h 15 min	++	−	+	−
H98	31	Male	7h	+	+	+	+
H61	36	Female	21h 19 min	+	−	+	−
H109	42	Male	8h 45 min	++	+	+	−
H87	55	Female	5h 50 min	+	−	+	−
H122	57	Female	12h 15 min	+	−	+	+
H107	65	Male	5h 20 min	+	−	−	−
H94	69	Female	5h 25 min	−	−	−	−
H114	75	Female	3h 30 min	++	−	+	+
H33	87	Female	3h 35 min	+	−	−	−
H55	86	Male	4h 45 min	+	+	+	++
H34	91	Female	3h 15 min	+	−	+	++

Key: STV, stria vascularis; RP, root process; OCT, organ of Corti; RC, Rosenthal's canal.

3. Results

3.1. Age-related auditory function declines in CBA/CaJ mice

CBA/CaJ mice have been widely used as a "normal aging" model in age-related hearing loss research (Henry and Chole, 1980; Ohlemiller et al., 2004; Sergeyenko et al., 2013; Zheng et al., 1999). Auditory brain stem responses (ABRs) were measured in young adult controls (n = 15) and aged mice (n = 12). As shown in Fig. 8, significant threshold shifts of 40–60 dB and greatly reduced maximum amplitudes were present in ABR wave I responses in the aged group at all frequencies tested (Student's unpaired *t*-test; $p < 0.001$). Sharp reductions of maximum amplitudes in ABR wave I responses indicate a decline in the suprathreshold hearing function and suggest a loss of auditory nerve activities (Hellstrom and Schmiedt, 1990; Lang et al., 2003). In addition, there was an EP reduction of about 20 mV in old ears compared with young controls (Fig. 8C; Mann-Whitney test; $p < 0.001$).

3.2. Age-related changes in ultrastructural morphology and neural crest cell–associated gene expression in the mouse cochlea

Several cochlear cell types are thought to derive from neural crest. Among them, intermediate cells in the STV are classified as neural crest–derived melanocytes because all stages of melanogenesis, including premelanosomes, melanosomes, and melanin granules, are found in these cells (Hilding and Ginzberg, 1977). Genetic mutations that deplete strial intermediate cells in developing mice result in abnormal strial development and a total loss of the EP (Steel and Barkway, 1989). Reductions in EP also occur when intermediate cells are selectively ablated in adult mice (Kim et al., 2013). Here we evaluated age-related ultrastructural changes in neural crest–derived cells in the cochlear lateral wall and auditory nerve of young adult (n = 6) and aged CBA/CaJ mice (n = 4). As shown in Fig. 1A, B and H, the extensive mitochondria-enriched cytoplasmic processes of the strial intermediate cells interdigitate tightly with the more electron-dense processes of marginal cells in young adult CBA/CaJ mice. Close apposition of the interdigital processes of intermediate cells with those of marginal cells is critical to proper exchange of ions across these membranes and EP generation (Hirose and Liberman, 2003; Schulte and Steel, 1994; Spicer et al., 2005). Structural alterations of intermediate cells in the aged mouse STV include partial to total loss of cellular processes (Fig. 1C, D and J) and the appearance of enlarged edematous spaces between intermediate and marginal cells (Fig. 1C, D and G). In the aged STV, abnormal intermediate cell processes in the absence of marginal cell processes often formed a swirl-like structure (Fig. 1I). To quantitatively evaluate age-related pathological alterations in the STV, we evaluated the areas of normal appearing intercellular interdigitations in the middle turns. The intermediate cell functional area was defined as the area occupied by interdigital intermediate cell processes as shown by shaded areas in Fig. 1H and I. A significant reduction (~a 50% loss) in the intermediate cell functional area was found in the aged cochleas (27 ± 6 μm^2 per 100 μm^2 STV) compared with young controls (52 ± 4 μm^2 per 100 μm^2 STV) (Mann-Whitney test; $p < 0.05$). Pathological alterations were also seen in the outer sulcus region in the spiral ligament of aged mice, including loss of the fibril-enriched matrix and accumulation of degenerative debris around RPs (Fig. 1F).

Satellite and Schwann cells in the peripheral auditory nerve are also thought to be of neural crest origin (Jessen and Mirsky, 2005;

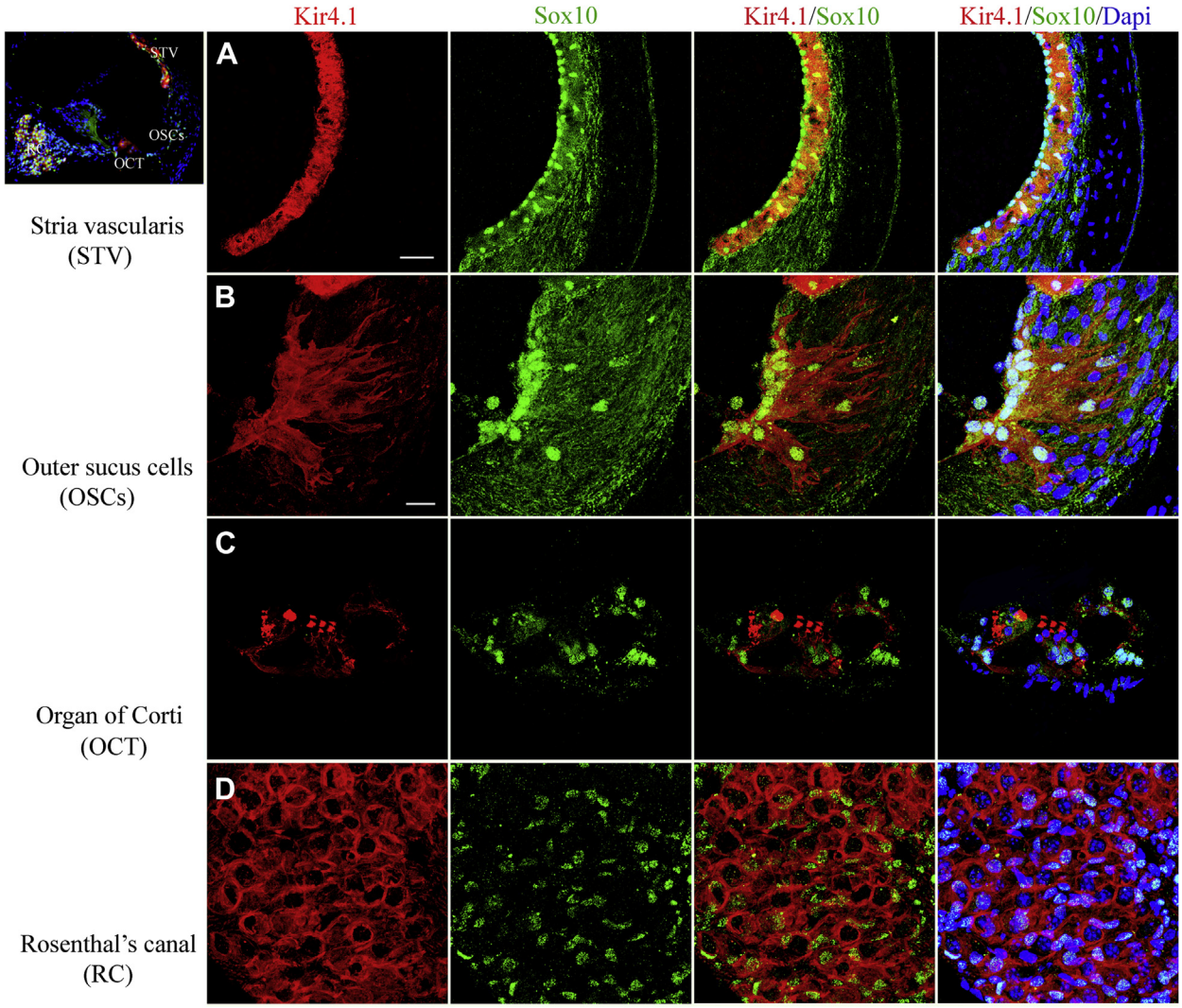

Fig. 2. Expression of Kir4.1 in neural crest–derived cells of the young adult mouse cochlea. Immunostaining patterns for Kir4.1 (red) and Sox10 (a neural crest–derived cell marker; green) are illustrated in the middle turn of a 2-month-old mouse. (A) Kir4.1 and Sox10 proteins were colocalized in the intermediate cells of the stria vascularis (STV). (B) Outer sulcus cells (OSCs) and their root processes also coexpressed Sox10 and Kir4.1. (C) Immunoreactive Kir4.1 and Sox10 were also found in supporting cells in the organ of Corti (OCT). (D) A honeycomb-like staining pattern for Kir4.1 is clearly shown by the $Sox10^{+}$ satellite cells ensheathing spiral ganglion neurons in Rosenthal's canal (RC). Nuclei were counterstained with Dapi (blue). Scale bars, 25 μm in A; 12 μm in B (applies to C and D). Abbreviation: Dapi, 4′,5-diamidino-2-phenylindole. (For interpretation of the references to color in this figure legend, the reader is referred to the Web version of this article.)

Woodhoo and Sommer, 2008). Evaluation of the auditory nerves from the same group of mice described previously revealed a number of age-related pathological alterations in the myelinating satellite cells ensheathing SGNs. These changes included disruption of myelin sheaths (Fig. 9D, H, I, K and L), the presence of multiple vacuoles in the intralamellar regions (Fig. 9D, F, I–K), electron-dense inclusion particles (Fig. 9H, J and K), myelin segmentation (Fig. 9F, G and J) and a separation between the external mesaxon members (Fig. 9D). Lipofuscin-like material aggregates were often seen in the cell bodies of SGNs in the aged mice (Fig. 9E). The accumulation of lipofuscin aggregates has been reported in aged neurons in numerous locations and is considered to be a hallmark of aging. (Moreno-García et al., 2018).

Age-related alterations in the expression pattern of neural crest–related genes were examined by microarray transcriptional profiling of lateral wall and auditory nerve preparations from young adult and aged CBA/CaJ mice. Differential expression analysis identified 53 and 50 neural crest–related genes that were expressed in an age-dependent manner in the cochlear lateral wall and auditory nerve, respectively (Figs. 1L and 9M; Supplementary Tables 1 and 2). A number of these differentially expressed genes, such as Cdh2, Ednrb, and Myl9, were downregulated in both the aged lateral wall and auditory nerve (Figs. 1M and 9N). Other genes were downregulated in one but not the other region. For example, Notch4, Sox5, Efnb1, Fgfr1, and Fgfr2 were selectively downregulated in the aged lateral wall, whereas Dix5, Sox9, Gfap, Mpz, and Olig1 were downregulated in the aged auditory nerve (Figs. 1M and 9N).

3.3. Kir4.1 expression in neural crest–derived cells in the mouse cochlea

Sox10 is a neural crest transcription factor with a conserved high-mobility group DNA-binding domain that plays important roles in differentiation and maintenance of melanocytes and peripheral glial cells (Herbarth et al., 1998; Britsch et al., 2001).

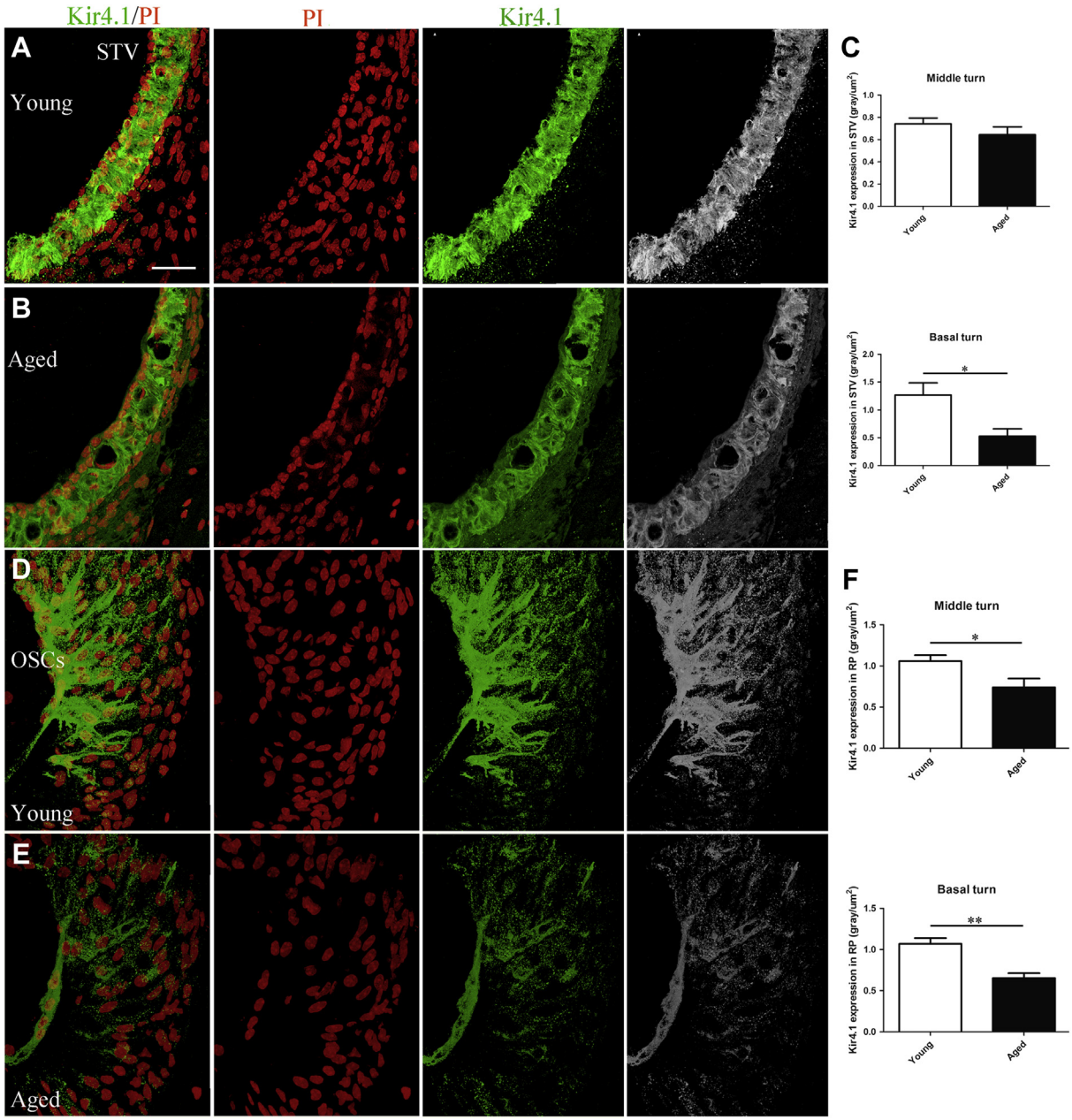

Fig. 3. Age-related reduction of Kir4.1 expression in the mouse cochlear lateral wall. (A-C) Semiquantitation of Kir4.1 expression levels in the STV as judged by measurements of fluorescence intensity in the middle and basal turns of the young versus aged group, revealed a significant decline in the basal but not the middle turns of aged mice. (D–F) Immunostaining for Kir4.1 also declined in OSC root processes of the spiral ligament. A significant reduction of Kir4.1 fluorescence intensity was found in both the middle and basal turns of the aged mice. Data are presented as mean ± SEM ($^{*}p < 0.05$, $^{**}p < 0.01$, Student's *t*-test, unpaired, 2-tailed; 5 mice for young adult group and 4 mice for aged group). Nuclei were counterstained with PI (red). Scale bar: 25 μm in A (applies to B-E). Abbreviations: OSC, outer sulcus cell; STV, stria vascularis. (For interpretation of the references to color in this figure legend, the reader is referred to the Web version of this article.)

Anti-Sox10 was used to label nuclei of cochlear neural crest–derived cells in dual staining experiments with Kir4.1 in the CBA/CaJ mouse cochlea (Fig. 2). In agreement with previous studies on the expression of Kir4.1 in animal models (Hibino et al., 1997; Ando et al., 1999; Rozengurt et al., 2003; Jagger et al., 2010; Kim et al., 2013), Kir4.1 immunoreactivity in the mouse cochlea was present in several cell types of neural crest origin including intermediate cells in the STV (Fig. 2A), outer sulcus cells in the spiral ligament (Fig. 2B), and satellite cells in the spiral ganglion (Fig. 2D). In addition, $Sox10^{+}$ supporting cells in the OCT expressed Kir4.1 as previously reported (Hibino et al., 1997).

3.4. Kir4.1 immunostaining in neural crest–derived cells undergoes alterations with age in the mouse cochlea

Cochlear Kir4.1 immunoreactivity was semiquantitatively analyzed by measuring relative fluorescence intensity of sections through the middle and basal turns of young and old mice. The intensity of Kir4.1 immunostaining was reduced in strial intermediate cells of the STV (Fig. 3A–C) and outer sulcus (Fig. 3D–F) in aged mice. The average pixel density of Kir4.1 expression in the STV of young versus aged mice was 0.74 and 0.64 gray/um^2 in the middle turn and 1.26 and 0.52 gray/um^2 in the basal turn, respectively (Fig. 3C). This reduction in Kir4.1 immunostaining pixel

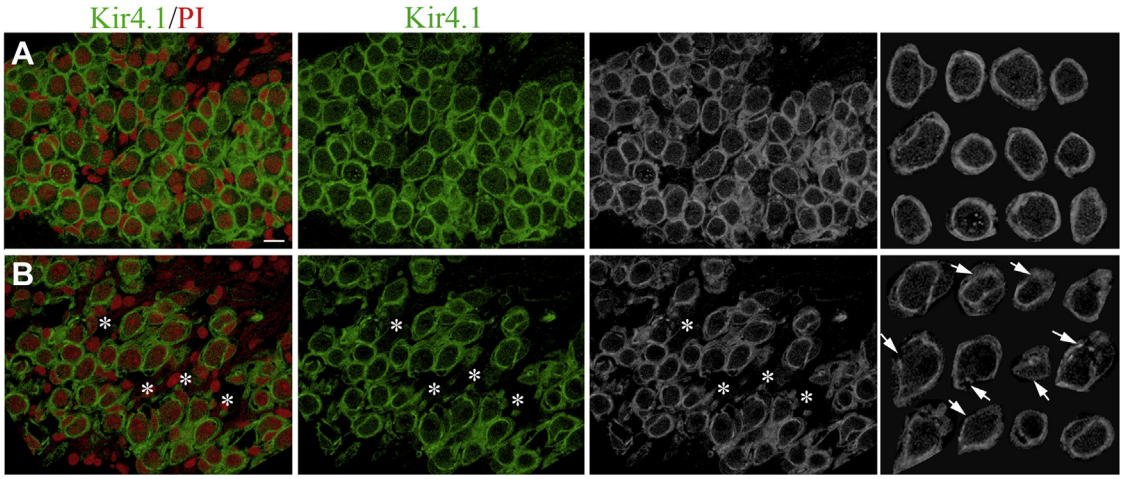

Fig. 4. Age-related alterations in the Kir4.1 immunostaining pattern in satellite cells. The honeycomb-like Kir4.1 expression pattern reflects satellite cells ensheathing SGNs in the basal turn of young (A) and aged (B) CBA/CaJ mice. Notable alterations in the immunostaining pattern for Kir4.1 were seen in satellite cells of aged mice including discontinuities and thinning of Kir4.1$^+$ components (arrows). The far right panels show regions randomly selected from images in the left panels. Nuclei were counterstained with PI (red). Scale bar: 8 μm in A (applies to B, except for the panels at far right). Abbreviations: PI, propidium iodide; SGN, spiral ganglion neuron. (For interpretation of the references to color in this figure legend, the reader is referred to the Web version of this article.)

density in aged mice was significant in the basal turn ($p < 0.05$) but not the middle turn. A reduction in the Kir4.1 immunostaining intensity was also seen in the outer sulcus region of aged mice (Fig. 3D and E). The average Kir4.1$^+$ pixel density in root cells in young and aged mice was 1.06 versus 0.74 gray/um^2 for the middle turn and 1.07 versus 0.65 gray/um^2 for the basal turn. These pixel densities in root cell processes were significantly different between the young and aged mice in both the middle and basal turns ($p < 0.05$ and <0.01, respectively) (Fig. 3F).

The number of SGNs is reduced in aged mice (Fig. 4A and B), in agreement with previous observations of CBA/CaJ mice at a similar age (Ohlemiller et al., 2010). A honeycomb-like Kir4.1$^+$ satellite cell staining pattern was present in the auditory nerve of both young and old mice (Fig. 4A and B). However, a slight but noticeable difference was seen in the immunostaining pattern of satellite cells in the aged spiral ganglion. These differences included discontinuity and thinning or blurred areas (Fig. 4B), which may also reflect structural changes in the myelin sheath

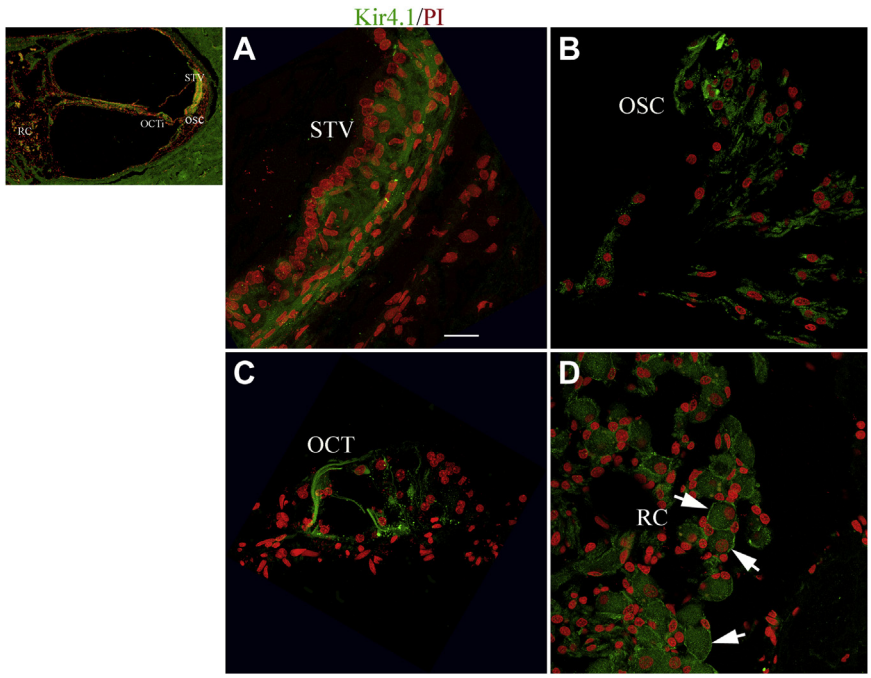

Fig. 5. Immunolocalization of Kir4.1 in the human cochlea. (A–D) Similar to the mouse, the Kir4.1 immunoactivity was present in cells of the STV (A), OSCs (B), support cells in the Organ of Corti (C) and satellite cells surrounding SGNs within RC (D, arrows). The cochlear sections were taken from an 86-year-old donor (A-D). Nuclei were counterstained with PI (red). Scale bar: 12 μm in A (applies to B-D). Abbreviations: OCT, Organ of Corti; OSC, Outer sulcus cells; PI, propidium iodide; RC, Rosenthal's canal; SGN, spiral ganglion neuron; STV, stria vascularis. (For interpretation of the references to color in this figure legend, the reader is referred to the Web version of this article.)

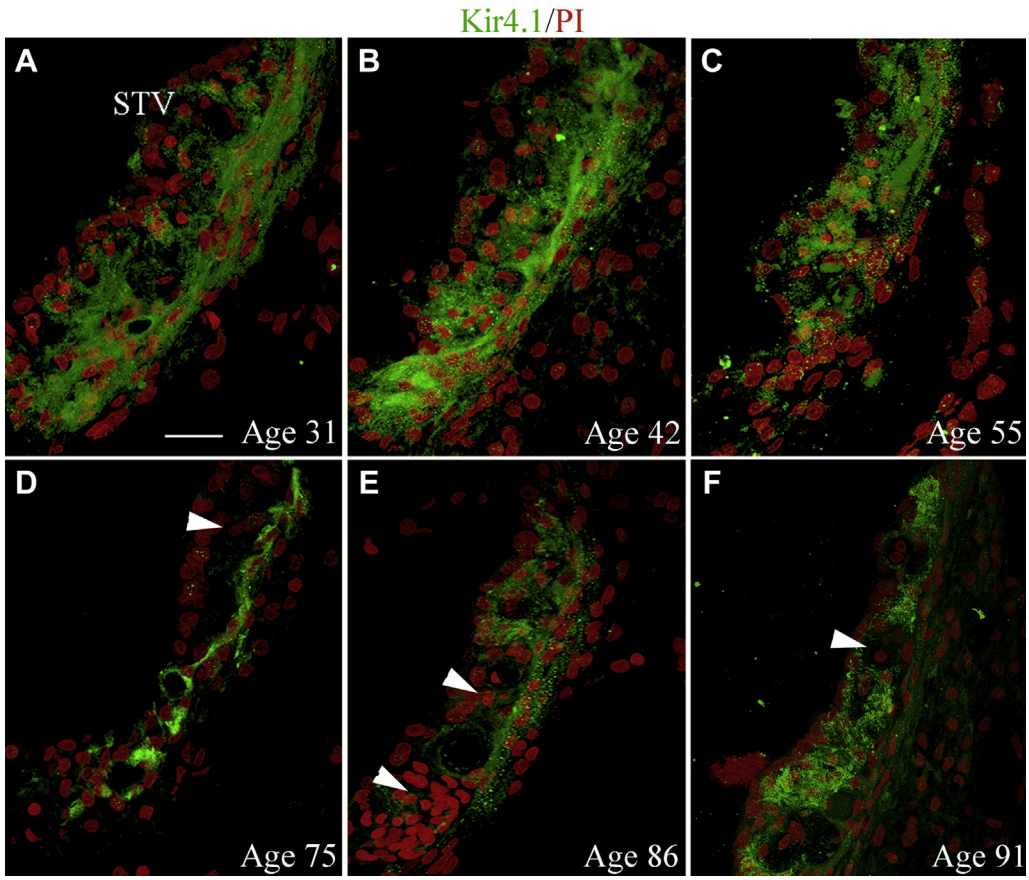

Fig. 6. Immunostaining patterns for Kir4.1 in the STV from 6 temporal bones of different ages. (A–F) Kir4.1 immunoreactivity for intermediate cells in the STV generally appeared stronger and more uniform in the ears from the 31-, 42-, and 55-year-old donors (A–C). (D–E) There was a partial loss or reduction of Kir4.1 immunoreactivity in the STV (arrowheads) of the 3 human temporal bones from the 75-, 86-, and 91-year-old donors. All images were taken from the middle turn of the cochlea. Nuclei were counterstained with PI (red). Scale bar: 12 μm in A (applies to B–F). Abbreviations: PI, propidium iodide; STV, stria vascularis. (For interpretation of the references to color in this figure legend, the reader is referred to the Web version of this article.)

formed by the satellite cells as reported in our previous study (Xing et al., 2012).

3.5. Kir4.1 expression in neural crest–derived cells of the human cochlea

As shown in Table 1, a total of 12 temporal bones from 7 female and 5 male donors aged from 30 to 91 years were examined in this study. The postmortem fixation interval ranged from around 3–21 hours. Immunoreactive Kir4.1 was present in HTBs in the same cell types as the mouse namely intermediate cells, outer sulcus cells, and satellite cells (Figs. 5–7). Fig. 6 depicts Kir4.1 immunostaining patterns in the STV of cochleas from middle-aged (younger than 55 year-old) and elderly (greater than 75 year old) donors. A notable reduction (or absence) of Kir4.1 immunoreactivity was present in some areas of the STV in the older ears (Fig. 6D–F). The finding that Kir4.1$^+$ regions in the STV appeared thinner in the older than the younger temporal bone is consistent with previous studies showing age-related progressive atrophy of the STV in HTBs (Suzuki et al., 2006).

In the auditory nerve, Kir4.1 immunoreactivity was also observed in satellite cells of the human cochleas examined (Fig. 7; Table 1). The percentage of SGNs ensheathed by Kir4.1$^+$ cells was determined in the middle and basal turns of these HTBs (Table 2) and ranged from 15%–32% in the middle turn and 19%–30% in the basal turn. The younger specimens (aged 31 and 57 years; Fig. 7A and B) had higher percentages of SGNs associated with Kir4.1$^+$ cells in the basal auditory nerve than did the older ears (aged 86 and 91 years; Fig. 7C and D). Because the postmortem interval between death and fixation was much longer in the younger as compared to the older specimens, we did not attempt to quantify these differences.

4. Discussion

In this study, we examined age-dependent alterations of Kir4.1 expression in neural crest–derived cells in the mouse and human cochlea. The data demonstrate that Kir4.1 immunoreactivity declines significantly with age in strial intermediate cells and outer sulcus cells and their root processes in the mouse cochlear lateral wall. Age-related changes in Kir4.1 immunostaining were also seen in satellite cells ensheathing SGNs in the mouse auditory nerve. However, these changes were less pronounced than those in the lateral wall and most probably were associated with neuronal cell loss with age. The distribution of Kir4.1 in the human cochlea was similar to that in the mouse. Age-related declines in immunostaining intensity appeared to be present in the STV but evaluation of more specimens will be required to confirm this and to determine if alterations in the staining patterns of satellite cells occur in older humans.

In the cochlear lateral wall, both strial intermediate cells and outer sulcus cells contribute to the maintenance of K^+ ion

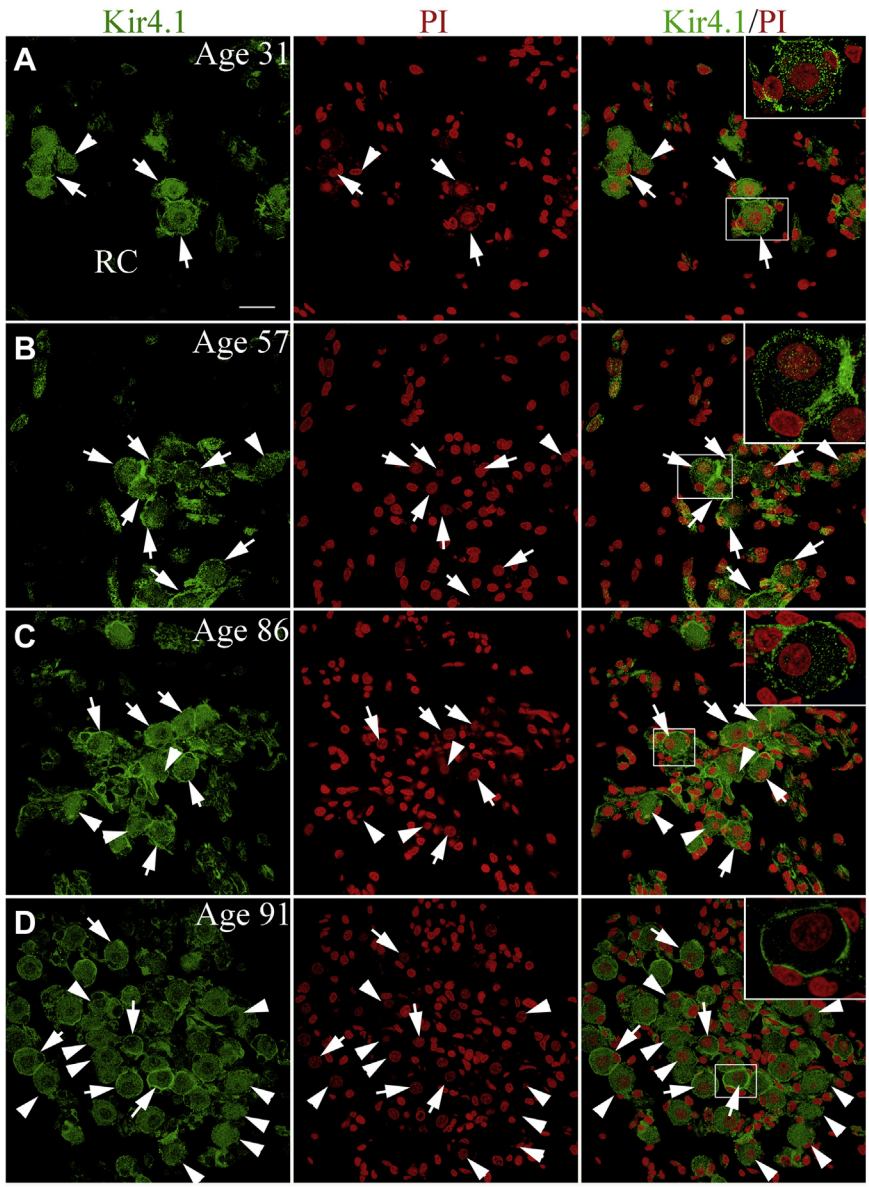

Fig. 7. Kir4.1 immunoreactivity in satellite cells of human spiral ganglion. (A, B) Kir4.1$^+$ satellite cells (arrows) around SGNs seen in the human temporal bones from a 31-year-old donor and a 57-year-old donor. Arrowheads point to SGNs devoid of Kir4.1$^+$ satellite cells. (C, D) An increase in Kir4.1$^-$ satellite cells was seen in sections from an 86- and 91-year-old donor. Additional information concerning the percentage of Kir4.1$^+$ satellite cells in the spiral ganglion from the younger and older donor groups is provided in Table 2. Nuclei were counterstained with PI (red). Scale bar: 10 μm in A (applies to B–F). Abbreviations: PI, propidium iodide; SGN, spiral ganglion neuron. (For interpretation of the references to color in this figure legend, the reader is referred to the Web version of this article.)

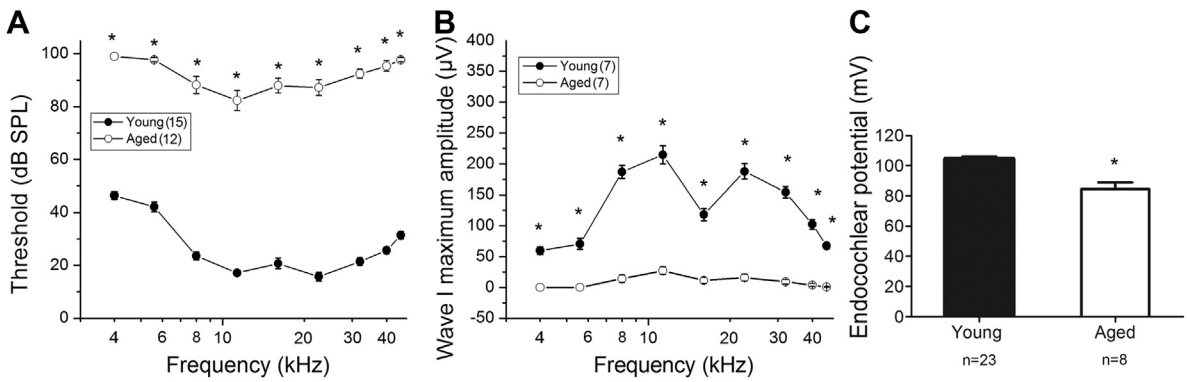

Fig. 8. Declines in auditory nerve function in aged CBA/CaJ mice. (A, B) ABR wave I thresholds were elevated, and maximum amplitudes were decreased in aged mice (2–2.5 years old) at all frequencies tested. Differences between young and old CBA/CaJ mice in wave I thresholds (A) and maximum amplitude (B) were significant at all frequencies (Student's unpaired *t*-test, $^*p < 0.001$). (C) An EP reduction was seen in aged compared with the young control group (Mann-Whitney test; $^*p < 0.001$). All data are presented as mean ± SEM. Abbreviations: ABR, auditory brain stem response; EP, endocochlear potential.

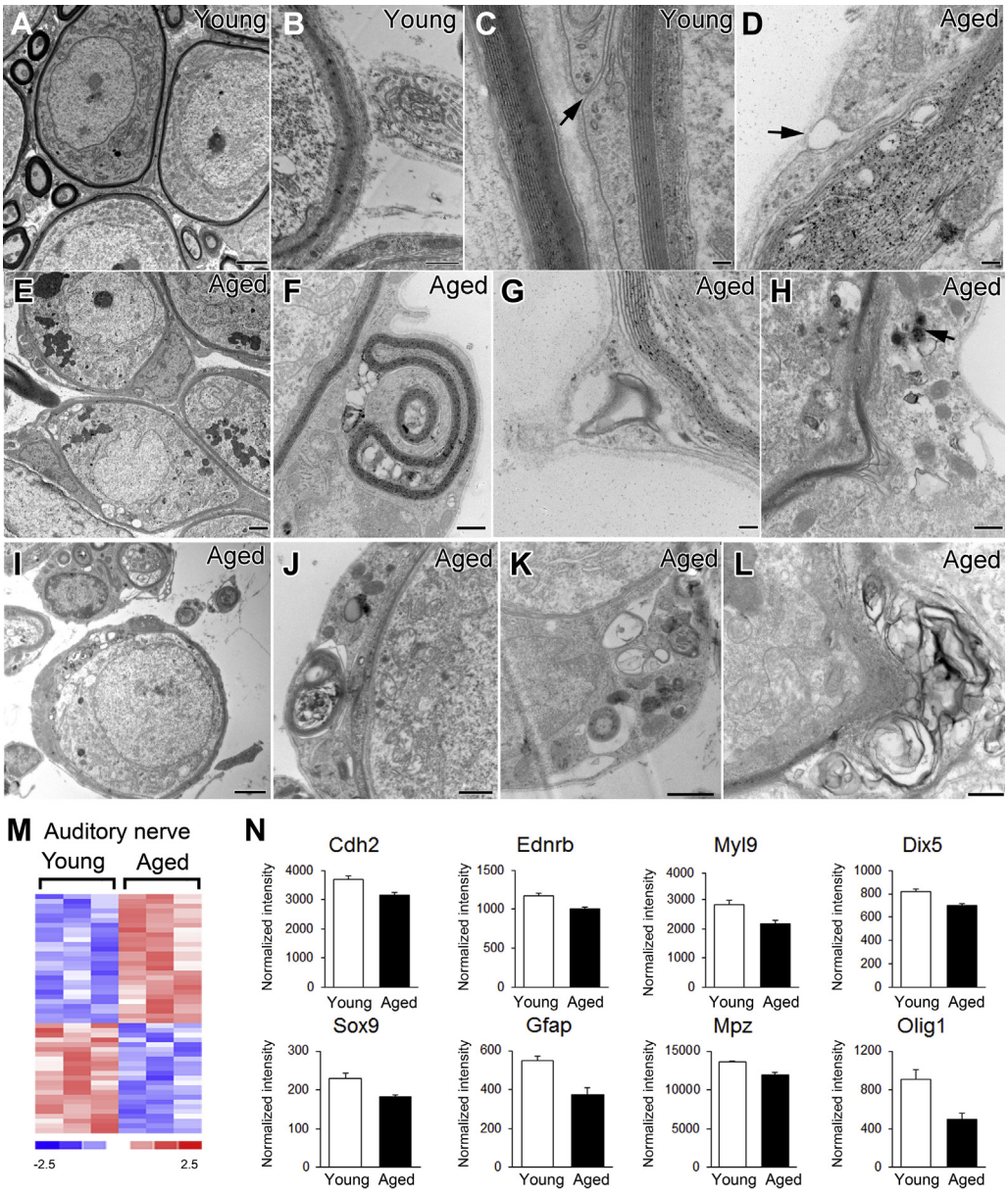

Fig. 9. Age-related ultrastructural alterations and changes in neural crest–associated gene expression patterns in the mouse auditory nerve. (A–C) Normal ultrastructural morphology of satellite cells ensheathing type I spiral ganglion neurons of young adult mice. Surrounding axons are enclosed by multiple layers of myelin and only narrow gaps are present between members of external mesaxons (arrow). (D–L) Pathological alterations in satellite cells of aged mice include enlarged spaces or vacuoles between myelin layers. Electron-dense cytoplasmic inclusions (an arrow in H, J, K), segmented myelin or myelin debris (F, G, I, J, K, L) and a separation of external mesaxon members (arrow in D). A cluster of lipofuscin-like bodies appears in the spiral ganglion neurons of aged mouse cochleas (E). (M) Heatmap of microarray data showing differential expression of 50 neural crest–related genes in the aged cochlear auditory nerve compared with young adult controls (genes scored $p < 0.05$; Student's *t*-test, unpaired, 2-tailed, not assuming equal variance). The false discovery rate for this comparison approximated 24%. (N) Expression values are shown for representative neural crest cell–associated genes in the auditory nerve. Scale bar: 2 μm in A, E, I; 500 nm in B, F, H, K, L; 100 nm in C, D, G; 800 nm in J.

Table 2
Percentages of SGNs with Kir4.1$^+$ cells in human cochleas

ID	Age	Sex	Death to perfusion interval	Percentage of SGNs with Kir4.1$^+$ cells (%)	
				Middle turn	Basal turn
H98	31	Male	7h	32.47	26.03
H122	57	Female	12h 35 min	15.32	30.44
H114	75	Female	3h 30 min	27.03	25.68
H55	86	Male	4h 45 min	23.14	24.24
H34	91	Female	3h 15 min	15.08	18.92

Key: SGN, spiral ganglion neuron.

homeostasis and recycling, which is needed for generation and maintenance of the EP (Jagger and Forge, 2012; Schulte and Steel, 1994; Spicer and Schulte, 1996; Wangemann, 2002). Unlike marginal and basal cells, intermediate cells are melanocytes of neural crest origin (Hilding and Ginzberg, 1977; Steel and Barkway, 1989). During development, intermediate cells migrate to the STV and, together with marginal cells, form a unique extracellular space termed the "intrastrial space" (Salt et al., 1987).

Pathological alteration such as edema were often seen in these intermediate cell–associated structures after acute cochlear injury such as ototoxic drug administration (Santi et al., 1985) or

noise exposure (Hirose and Liberman, 2003). The Kir4.1 channels located in the apical membrane of intermediate cells are needed to keep a very low K^+ concentration within the intrastrial space while maintaining a high K^+ concentration within the intermediate cells, both of which are critical for generation and maintenance of the EP in this compartment (Hibino and Kurachi, 2006; Wangemann, 2002). Unlike the well-studied strial cells in the lateral wall, the function of outer sulcus cells in the spiral ligament is less well understood (Jagger and Forge, 2012; Shodo et al., 2017). These cells are connected by tight junctions apically and together form a multicellular branched epithelial structure similar to the roots of a tree. The root-like processes project into the spiral ligament where they are surrounded by and closely associated with type 2 fibrocytes and their numerous cellular processes (Galic and Giebel, 1989; Kimura, 1984; Spicer and Schulte, 1996). The expression of Kir4.1 in outer sulcus cells and their root processes was first reported in the guinea pig by Jagger et al. (2010) and later in rat and human cochlea by Eckhard et al. (2012). A three-dimensional reconstruction study has confirmed that the root processes provide an enlarged basolateral cell surface area in close apposition to type 2 fibrocytes, allowing more efficient exchange of K^+ in the lateral wall (Shodo et al., 2017). The number and size of individual root processes increases from the apex to the base of the cochlea, along with the increased volume density of type 2 fibrocytes, theoretically supporting the greater level of K^+ reabsorption needed in the higher frequency encoding regions (Galic and Giebel, 1989; Jagger et al., 2010; Jagger and Forge, 2012; Kimura, 1984; Spicer and Schulte, 1996). Our results revealed that both strial intermediate cells and outer sulcus cells stain positively for Sox10, a marker of neural crest–derived cells. This coexpression of Sox10 and Kir4.1 in the outer sulcus strongly suggests that similar to strial intermediate cells, they play an important role in K^+ circulation and maintenance of the EP.

Age-related atrophy of the STV has been documented in animal models (Gratton and Schulte, 1995; Ohlemiller, 2009; Schulte and Schmiedt, 1992) and in HTBs (Schuknecht et al., 1974; Schuknecht and Gacek, 1993). Ultrastructural examination has also revealed degeneration of strial marginal, intermediate and basal cells in cochleas obtained from older human donors (Takahashi, 1971). Although marginal cells have long been considered as the prime target for degenerative changes in the aged cochlear lateral wall, a combination of marginal and intermediate cell degeneration and/or loss is frequently seen in the late phases of strial atrophy (Thomopoulos et al., 1997; Spicer and Schulte, 2005; Ohlemiller et al., 2010; Hao et al., 2014). The results presented here demonstrating declines in immunostaining for Kir4.1 with age in both strial intermediate and outer sulcus cells, together with quantitative analysis of an age-related decrease in the intermediate cell functional area suggests that both of these cell types, although they may act independently, play a major role in lateral wall K^+ homeostasis. Together, these observations indicate that age-dependent dysfunction of at least 2 different populations of neural crest–derived cells is associated with the EP reduction in the aged CBA/CaJ mouse model of presbyacusis, as shown in this study (Fig. 8C) and a previous study (Ohlemiller et al., 2010). Pathophysiological alterations of neural crest–derived cells in the lateral wall may also contribute to the declines of auditory nerve function seen in animal models of metabolic presbyacusis (the strial form of presbyacusis) as demonstrated in previous studies (Lang et al., 2003; Schmiedt, 2009). Chronic mild to moderate reductions in the EP have been shown to decrease auditory nerve activity, particularly the activity of low spontaneous rate fibers, which is the key auditory nerve fiber subpopulation contributing to the suprathreshold functions of the auditory nerve (Schmiedt, 2009).

Another interesting, but not totally unexpected, finding of this study was the age-related change in Kir4.1 immunostaining patterns of satellite cells ensheathing SGNs in both mouse and human cochleas. Mutations in the Kir4.1 (KCNJ10) gene have been linked to a wide range of neurological diseases, such as SeSAME/EAST syndrome (including sensorineural hearing loss), epilepsy, and autism spectrum disorders. Evidence is accumulating that Kir4.1 activity contributes to several key functions of glial cells in the central nervous system, including the control of resting and hyperpolarized membrane potentials, the maintenance of K^+ homeostasis, and the regulation of cell volume and glutamate uptake (Guglielmi et al., 2015; Milton and Smith, 2018; Nwaobi et al., 2016). K^+ released during neuronal activity is taken up by nearby glial cells via Kir4.1 channels and then extruded from glia into extracellular sinks. The initiation and growth of Kir channel activity was found to be coincident with the maturation of glial cell populations (Butt and Kalsi, 2006; Newman, 1985; Sontheimer et al., 1989). In certain pathological conditions such as injury to the trigeminal ganglion or spinal cord, decreases in Kir4.1 channel activity cause changes in neuronal excitability, which may lead to abnormal sensory perception and the death of motor neurons (Kaiser et al., 2006; Vit et al., 2008). Here, our data show age-dependent alterations in Kir4.1 expression in satellite, but not Schwann cells, in both the mouse and human auditory nerve. These results, together with the demonstration of ultrastructural abnormalities in satellite cells, imply that dysfunction of cochlear glial cells plays a role in abnormal function of the auditory nerve with age and is a contributing factor to neural presbyacusis.

At least 3 types of human presbyacusis have been described based primarily on pathological changes in specific cell types in the cochlea. They are termed (1) sensory, mainly involving sensory hair cells and supporting cells in the OCT; (2) neural, demonstrated by the loss of neurons or their peripheral processes in the auditory nerve; and (3) strial (metabolic), as a result of the loss/dysfunction of cells within the cochlear lateral wall (Schuknecht et al., 1974; Schuknecht and Gacek, 1993). The findings reported here show that abnormalities of Kir4.1 expression can occur with age in several types of nonsensory cells of neural crest origin in different regions of the cochlea. Together, these observations provide a cellular basis for the pathophysiological processes associated with both metabolic and neural phenotypes of presbyacusis, which have often been observed together and are most likely to occur as a mixed phenotype.

5. Conclusion

Age-related changes in Kir4.1 immunoreactivity were identified in 3 different cell types of neural crest origin residing in the lateral wall and spiral ganglion of both the mouse and human cochlea. The results reveal that degeneration/dysfunction of these nonsensory cells in the cochlea is associated with the onset of both metabolic and neural forms of presbyacusis. These observations also support previous studies indicating that 2 or more forms of presbyacusis can coexist in the same ear.

Disclosure

The authors declare no competing financial interests.

Acknowledgements

This work has been supported (in part) by National Institutes of Health Grants R01DC012058 (HL), R56DC012058 (HL) P50DC00422 (HL, BAS), P30 CA138313, and S10 OD018113 from the Cell & Molecular Imaging Shared Resource and Hollings Cancer Center, and

C06 RR014516 from the Extramural Research Facilities Program of the National Center for Research Resources. The project also received support from the South Carolina Clinical and Translational Research (SCTR) Institute with an academic home at the Medical University of South Carolina, NIH/NCRR Grant number UL1RR029882. Microarray experimentation conducted at the MUSC Proteogenomics Facility was supported by NIGMS GM103499 and MUSC's Office of the Vice President for Research. The authors thank Juhong Zhu, Nancy Smythe, Reycel Rodriguez, and Linda McCarson for their excellent technical assistance.

Appendix A. Supplementary data

Supplementary data to this article can be found online at https://doi.org/10.1016/j.neurobiolaging.2019.04.009.

References

Ando, M., Takeuchi, S., 1999. Immunological identification of an inward rectifier K+ channel (Kir4.1) in the intermediate cell (melanocyte) of the cochlear stria vascularis of gerbils and rats. Cell Tissue Res. 298, 179–183.

Ashburner, M., Ball, C.A., Blake, J.A., Botstein, D., Butler, H., Cherry, J.M., Davis, A.P., Dolinski, K., Dwight, S.S., Eppig, J.T., Harris, M.A., Hill, D.P., Issel-Tarver, L., Kasarskis, A., Lewis, S., Matese, J.C., Richardson, J.E., Ringwald, M., Rubin, G.M., Sherlock, G., 2000. Gene ontology: tool for the unification of biology. The Gene Ontology Consortium. Nat. Genet. 25, 25–29.

Bond, C.T., Pessia, M., Xia, X.M., Lagrutta, A., Kavanaugh, M.P., Adelman, J.P., 1994. Cloning and expression of a family of inward rectifier potassium channels. Receptors Channels 2, 183–191.

Britsch, S., Goerich, D.E., Riethmacher, D., Peirano, R.I., Rossner, M., Nave, K.A., Birchmeier, C., Wegner, M., 2001. The transcription factor Sox10 is a key regulator of peripheral glial development. Genes Dev. 15, 66–78.

Butt, A.M., Kalsi, A., 2006. Inwardly rectifying potassium channels (Kir) in central nervous system glia: a special role for Kir4.1 in glial functions. J. Cell Mol. Med. 10, 33–44.

Chen, J., Zhao, H.B., 2014. The role of an inwardly rectifying K(+) channel (Kir4.1) in the inner ear and hearing loss. Neuroscience 265, 137–146.

Cunningham, C.D., Schulte, B.A., Bianchi, L.M., Weber, P.C., Schmiedt, B.N., 2001. Microwave decalcification of human temporal bones. Laryngoscope 111, 278–282.

Cui, Y., Yang, Y., Ni, Z., Dong, Y., Cai, G., Foncelle, A., Ma, S., Sang, K., Tang, S., Li, Y., Shen, Y., Berry, H., Wu, S., Hu, H., 2018. Astroglial Kir4.1 in the lateral habenula drives neuronal bursts in depression. Nature 554, 323–327.

Dupin, E., Sommer, L., 2012. Neural crest progenitors and stem cells: from early development to adulthood. Dev. Biol. 366, 83–95.

Eckhard, A., Gleiser, C., Rask-Andersen, H., Arnold, H., Liu, W., Mack, A., Müller, M., Löwenheim, H., Hirt, B., 2012. Co-localisation of Kir4.1 and AQP4 in rat and human cochleae reveals a gap in water channel expression at the transduction sites of endocochlear K(+) recycling routes. Cell Tissue Res. 350, 27–43.

Galic, M., Giebel, W., 1989. An electron microscopic study of the function of the root cells in the external spiral sulcus of the cochlea. Acta Otolaryngol. Suppl. 461, 1–15.

Garcia, M.A., Meca, R., Leite, D., Boim, M.A., 2007. Effect of renal ischemia/reperfusion on gene expression of a pH-sensitive K+ channel. Nephron Physiol. 106, 1–7.

Gates, G.A., Mills, J.H., 2005. Presbycusis. Lancet 366, 1111–1120.

Gratton, M.A., Schulte, B.A., 1995. Alterations in microvasculature are associated with atrophy of the stria vascularis in quiet-aged gerbils. Hear. Res. 82, 44–52.

Guglielmi, L., Servettini, I., Caramia, M., Catacuzzeno, L., Franciolini, F., D'Adamo, M.C., Pessia, M., 2015. Update on the implication of potassium channels in autism: K(+) channelautism spectrum disorder. Front. Cell Neurosci. 9, 34.

Gupta, R.K., Prasad, S., 2013. Early down regulation of the glial Kir4.1 and GLT-1 expression in pericontusional cortex of the old male mice subjected to traumatic brain injury. Biogerontology 14, 531–541.

Hao, X., Xing, Y., Moore, M.W., Zhang, J., Han, D., Schulte, B.A., Dubno, J.R., Lang, H., 2014. Sox10 expressing cells in the lateral wall of the aged mouse and human cochlea. PLoS One 9, e97389.

Hellstrom, L.I., Schmiedt, R.A., 1990. Compound action potential input/output functions in young and quiet-aged gerbils. Hear. Res. 50, 163–174.

Herbarth, B., Pingault, V., Bondurand, N., Kuhlbrodt, K., Hermans-Borgmeyer, I., Puliti, A., Lemort, N., Goossens, M., Wegner, M., 1998. Mutation of the Sry-related Sox10 gene in Dominant megacolon, a mouse model for human Hirschsprung disease. Proc. Natl. Acad. Sci. U. S. A. 95, 5161–5165.

Henry, K.R., Chole, R.A., 1980. Genotypic differences in behavioral, physiological and anatomical expressions of age-related hearing loss in the laboratory mouse. Audiology 19, 369–383.

Hibino, H., Horio, Y., Inanobe, A., Doi, K., Ito, M., Yamada, M., Gotow, T., Uchiyama, Y., Kawamura, M., Kudo, T., Kurachi, Y., 1997. An ATP-dependent inwardly rectifying potassium channel, KAB-2 (Kir4.1), in cochlear stria vascularis of inner ear: its specific subcellular localization and correlation with the formation of endocochlear potential. J. Neurosci. 17, 4711–4721.

Hibino, H., Kurachi, Y., 2006. Molecular and physiological bases of the K+ circulation in the mammalian inner ear. Physiology (Bethesda) 21, 336–345.

Hilding, D.A., Ginzberg, R.D., 1977. Pigmentation of the stria vascularis. The contribution of neural crestmelanocytes. Acta Otolaryngol. 84, 24–37.

Hirose, K., Liberman, M.C., 2003. Lateral wall histopathology and endocochlear potential in the noise-damaged mouse cochlea. J. Assoc. Res. Otolaryngol. 4, 339–352.

Irizarry, R.A., Hobbs, B., Collin, F., Beazer-Barclay, Y.D., Antonellis, K.J., Scherf, U., Speed, T.P., 2003. Exploration, normalization, and summaries of high density oligonucleotide array probe level data. Biostatistics 4, 249–264.

Jagger, D.J., Forge, A., 2012. The enigmatic root cell - emerging roles contributing to fluid homeostasis within the cochlear outer sulcus. Hear. Res. 303, 1–11.

Jagger, D.J., Nevill, G., Forge, A., 2010. The membrane properties of cochlear root cells are consistent with roles in potassium recirculation and spatial buffering. J. Assoc. Res. Otolaryngol. 11, 435–448.

Jessen, K.R., Mirsky, R., 2005. The origin and development of glial cells in peripheral nerves. Nat. Rev. Neurosci. 6, 671–682.

Kaiser, M., Maletzki, I., Hulsmann, S., Holtmann, B., Schulz-Schaeffer, W., Kirchhoff, F., Bahr, M., Neusch, C., 2006. Progressive loss of a glial potassium channel (KCNJ10) in the spinal cord of the SOD1(G93A) transgenic mouse model of amyotrophic lateral sclerosis. J. Neurochem. 99, 900–912.

Kim, H.J., Gratton, M.A., Lee, J.H., Perez Flores, M.C., Wang, W., Doyle, K.J., Beermann, F., Crognale, M.A., Yamoah, E.N., 2013. Precise toxigenic ablation of intermediate cells abolishes the "battery" of the cochlear duct. J. Neurosci. 33, 14601–14606.

Kimura, R.S., 1984. Sensory and accessory epithelia of the cochlea. In: Friedmann, I., Ballantyne, J. (Eds.), Ultrastructural Atlas of the Inner Ear. Butterworths, London, pp. 101–132.

Kusunoki, T., Cureoglu, S., Schachern, P.A., Baba, K., Kariya, S., Paparella, M.M., 2004. Age-related histopathologic changes in the human cochlea: a temporal bone study. Otolaryngol. Head Neck Surg. 131, 897–903.

Lang, H., Li, M., Kilpatrick, L.A., Zhu, J., Samuvel, D.J., Krug, E.L., Goddard, J.C., 2011. Sox2 upregulation and glial cell proliferation following degeneration of spiral ganglion neurons in the adult mouse inner ear. J. Assoc. Res. Otolaryngol. 12, 151–171.

Lang, H., Schulte, B.A., Schmiedt, R.A., 2003. Effects of chronic furosemide treatment and age on cell division in the adult gerbil inner ear. J. Assoc. Res. Otolaryngol. 04, 164–175.

Lang, H., Jyothi, V., Smythe, N.M., Dubno, J.R., Schulte, B.A., Schmiedt, R.A., 2010. Chronic reduction of endocochlear potential reduces auditory nerve activity: further confirmation of an animal model of metabolic presbyacusis. J. Assoc. Res. Otolaryngol. 11, 419–434.

Lang, H., Xing, Y., Brown, L.N., Samuvel, D.J., Panganiban, C.H., Havens, L.T., Balasubramanian, S., Wegner, M., Krug, E.L., Barth, J.L., 2015. Neural stem/progenitor cell properties of glial cells in the adult mouse auditory nerve. Sci. Rep. 5, 13383.

Li, C., Wong, W.H., 2001. Model-based analysis of oligonucleotide arrays: expression index computation and outlier detection. Proc. Natl. Acad. Sci. U. S. A. 98, 31–36.

Lioy, D.T., Garg, S.K., Monaghan, C.E., Raber, J., Foust, K.D., Kaspar, B.K., Hirrlinger, P.G., Kirchhoff, F., Bissonnette, J.M., Ballas, N., Mandel, G., 2011. A role for glia in the progression of Rett's syndrome. Nature 475, 497–500.

Locher, H., de Groot, J.C., van Iperen, L., Huisman, M.A., Frijns, J.H., Chuva de Sousa Lopes, S.M., 2014. Distribution and development of peripheral glial cells in the human fetal cochlea. PLoS One 9, e88066.

Makary, C.A., Shin, J., Kujawa, S.G., Liberman, M.C., Merchant, S.N., 2011. Age-related primary cochlear neuronal degeneration in human temporal bones. J. Assoc. Res. Otolaryngol. 12, 711–717.

Milton, M., Smith, P.D., 2018. It's all about timing: the involvement of Kir4.1 channel regulation in acute ischemic stroke pathology. Front. Cell Neurosci. 12, 36.

Moreno-García, A., Kun, A., Calero, O., Medina, M., Calero, M., 2018. An overview of the role of lipofuscin in age-related neurodegeneration. Front. Neurosci. 12, 464.

Newman, E.A., 1985. Voltage-dependent calcium and potassium channels in retinal glial cells. Nature 317, 809–811.

Nwaobi, S.E., Cuddapah, V.A., Patterson, K.C., Randolph, A.C., Olsen, M.L., 2016. The role of glial-specific Kir4.1 in normal and pathological states of the CNS. Acta Neuropathol. 132, 1–21.

Ohlemiller, K.K., Gagnon, P.M., 2004. Apical-to-basal gradients in age-related cochlear degeneration and their relationship to "primary" loss of cochlear neurons. J. Comp. Neurol. 479, 103–116.

Ohlemiller, K.K., 2009. Mechanisms and genes in human strial presbycusis from animal models. Brain Res. 1277, 70–83.

Ohlemiller, K.K., Dahl, A.R., Gagnon, P.M., 2010. Divergent aging characteristics in CBA/J and CBA/CaJ mouse cochleae. J. Assoc. Res. Otolaryngol. 11, 605–623.

Panganiban, C.H., Barth, J.L., Darbelli, L., Xing, Y., Zhang, J., Li, H., Noble, K.V., Liu, T., Brown, L.N., Schulte, B.A., Richard, S., Lang, H., 2018. Noise-induced dysregulation of Quaking RNA binding proteins contributes to auditory nerve demyelination and hearing loss. J. Neurosci. 38, 2551–2556.

Rozengurt, N., Lopez, I., Chiu, C.S., Kofuji, P., Lester, H.A., Neusch, C., 2003. Time course of inner ear degeneration and deafness in mice lacking the Kir4.1 potassium channel subunit. Hear. Res. 177, 71–80.

Salt, A.N., Melichar, I., Thalmann, R., 1987. Mechanisms of endocochlear potential generation by stria vascularis. Laryngoscope 97, 984–991.

Santi, P.A., Lakhani, B.N., Edwards, L.B., Morizono, T., 1985. Cell volume density alterations within the stria vascularis after administration of a hyperosmotic agent. Hear. Res. 18, 283–290.
Schmiedt, R.A., 1996. Effects of aging on potassium homeostasis and the endocochlear potential in the gerbil cochlea. Hear. Res. 102, 125–132.
Schmiedt, R.A., Mills, J.H., Boettcher, F.A., 1996. Age-related loss of activity of auditory-nerve fibers. J. Neurophysiol. 76, 2799–2803.
Schmiedt, R.A., 2009. The physiology of cochlear presbyacusis. In: Gordon-Salant, S., Frisina, R.D., Poper, A.N., Fay, R.R. (Eds.), The aging auditory system: perceptual characterization and neural bases of presbyacusis. Springer, New York.
Schuknecht, H., 1968. Temporal bone removal at autopsy. Preparation and uses. Arch. Otolaryngol. 87, 129–137.
Schuknecht, H.F., Gacek, M.R., 1993. Cochlear pathology in presbyacusis. Ann. Otol Rhinol Laryngol. 102 (1 Pt 2), 1–16.
Schuknecht, H.F., Watanuki, K., Takahashi, T.T., Belal Jr., A.A., Kimura, R.S., Jones, D.D., Ota, C.Y., 1974. Atrophy of the stria vascularis, a common cause for hearing loss. Laryngoscope 84, 1777–1821.
Schulte, B.A., Schmiedt, R.A., 1992. Lateral wall Na,K-ATPase and endocochlear potentials decline with age in quiet-reared animals. Hear. Res. 61, 35–46.
Schulte, B.A., Steel, K.P., 1994. Expression of alpha and beta subunit isoforms of Na,K-ATPase in the mouse inner ear and changes with mutations at the Wv or Sid loci. Hear. Res. 78, 65–76.
Sergeyenko, Y., Lall, K., Liberman, M.C., Kujawa, S.G., 2013. Age-related cochlear synaptopathy: an early-onset contributor to auditory functional decline. J. Neurosci. 33, 13686–13694.
Shieh, C.C., Coghlan, M., Sullivan, J.P., Gopalakrishnan, M., 2000. Potassium channels: molecular defects, diseases, and therapeutic opportunities. Pharmacol. Rev. 52, 557–594.
Shodo, R., Hayatsu, M., Koga, D., Horii, A., Ushiki, T., 2017. Three-dimensional reconstruction of root cells and interdental cells in the rat inner ear by serial section scanning electron microscopy. Biomed. Res. 38, 239–248.
Slenter, D.N., Kutmon, M., Hanspers, K., Riutta, A., Windsor, J., Nunes, N., Mélius, J., Cirillo, E., Coort, S.L., Digles, D., Ehrhart, F., Giesbertz, P., Kalafati, M., Martens, M., Miller, R., Nishida, K., Rieswijk, L., Waagmeester, A., Eijssen, L.M.T., Evelo, C.T., Pico, A.R., Willighagen, E.L., 2018. WikiPathways: a multifaceted pathway database bridging metabolomics to other omics research. Nucleic Acids Res. 46, D661–D667.
Sontheimer, H., Trotter, J., Schachner, M., Kettenmann, H., 1989. Channel expression correlates with differentiation stage during the development of oligodendrocytes from their precursor cells in culture. Neuron 2, 1135–1145.
Spicer, S.S., Schulte, B.A., 1996. The fine structure of spiral ligament cells relates to ion return to the stria and varies with place-frequency. Hear. Res. 100, 80–100.
Spicer, S.S., Schulte, B.A., 2005. Pathologic changes of presbycusis begin in secondary processes and spread to primary processes of strial marginal cells. Hear. Res. 205, 225–240.
Steel, K.P., Barkway, C., 1989. Another role for melanocytes: their importance for normal stria vascularis development in the mammalian inner ear. Development 107, 453–463.
Suzuki, T., Nomoto, Y., Nakagawa, T., Kuwahata, N., Ogawa, H., Suzuki, Y., Ito, J., Omori, K., 2006. Age-dependent degeneration of the stria vascularis in human cochleae. Laryngoscope 116, 1846–1850.
Takahashi, T., 1971. The ultrastructure of the pathologic stria vascularis and spiral prominence in man. Ann. Otol. Rhinol. Laryngol. 80, 721–735.
The Gene Ontology Consortium, 2017. Expansion of the gene ontology knowledgebase and resources. Nucleic Acids Res. 45, D331–D338.
Thomopoulos, G.N., Spicer, S.S., Gratton, M.A., Schulte, B.A., 1997. Age-related thickening of basement membrane in stria vascularis capillaries. Hear. Res. 111, 31–41.
Tong, X., Ao, Y., Faas, G.C., Nwaobi, S.E., Xu, J., Haustein, M.D., Anderson, M.A., Mody, I., Olsen, M.L., Sofroniew, M.V., Khakh, B.S., 2014. Astrocyte Kir4.1 ion channel deficits contribute to neuronal dysfunction in Huntington's disease model mice. Nat. Neurosci. 17, 694–703.
Vit, J.P., Ohara, P.T., Bhargava, A., Kelley, K., Jasmin, L., 2008. Silencing the Kir4.1 potassium channel subunit in satellite glial cells of the rat trigeminal ganglion results in pain-like behavior in the absence of nerve injury. J. Neurosci. 28, 4161–4171.
Wangemann, P., 2002. K+ cycling and the endocochlear potential. Hear. Res. 165, 1–9.
Woodhoo, A., Sommer, L., 2008. Development of the Schwann cell lineage: from the neural crest to the myelinated nerve. Glia 56, 1481–1490.
Xing, Y., Samuvel, D.J., Stevens, S.M., Dubno, J.R., Schulte, B.A., Lang, H., 2012. Age-related changes of myelin basic protein in mouse and human auditory nerve. PLoS One 7, e34500.
Yamasoba, T., Kondo, K., Miyajima, C., Suzuki, M., 2003. Changes in cell proliferation in rat and Guinea pig cochlea after aminoglycoside-induced damage. Neurosci. Lett. 347, 171–174.
Zheng, Q.Y., Johnson, K.R., Erway, L.C., 1999. Assessment of hearing in 80 inbred strains of mice by ABR threshold analyses. Hear. Res. 130, 94–107.